

Quantum information processing device analysis based on quantum metrology

Mark J. Kandula, and Pieter Kok

Department of Physics and Astronomy, University of Sheffield, Sheffield S3 7RH, United Kingdom
May 24, 2022

Physical implementations of quantum information processing devices are generally not unique, and we are faced with the problem of choosing the best implementation. Here, we consider how different implementations are sensitive to variations in their components. To measure this, we adopt a quantum metrological approach, and find that the sensitivity of a device to variations in a component has a particularly simple form. We give two practical examples of sensitivities of quantum devices to variations in beam splitter transmittivities: the KLM and Reverse nonlinear sign gates for linear optical quantum computing with photonic qubits, and the enhanced optical Bell detectors by Grice and Ewert & van Loock. We find that for these Bell detectors, the design that uses fewer components performs better than the design with overall lower sensitivity to component variations.

1 Introduction

Quantum technologies promise dramatic improvements in computation, sensing, and communication, and many efforts are underway to develop it into a mature technology. One of the general challenges is that quantum devices typically need to be extraordinarily precise. We know from quantum fault tolerance theory that models with uncorrelated gate, propagation, and measurement errors may have an error rate of 0.75% per element [1], and it is not known whether more forgiving thresholds exist for equally realistic error models. The tolerances in quantum communication devices are likely less severe, but quantum sensing models are again known to be very susceptible to imperfections in the implementation [2]. This means that these quantum devices must be fabricated to a very high standard.

The precision of a device is usually specified in terms of the *fidelity*, which measures how much the actual output state of a device deviates from the intended (ideal) output state. In cases where the ideal output state is pure, the fidelity can be interpreted as the probability of mistaking the actual output state for the ideal output state [3]. It was shown by Myerson *et al.* that a single-shot readout of a qubit in an ion trap can be read out with 99.99% fidelity [4], and single- and two-qubit gates can achieve fidelities of 99.99% and 99.9%, respectively [5]. In other implementations, similar fidelities have been achieved [6]. A general method for calculating the fidelity of quantum operations was given by Pedersen *et al.* [7], and there is a sizeable literature on measuring deviations from ideal operations using various mathematical techniques [8–10].

In this paper, we propose a method for testing the sensitivity of quantum devices that is not based on the fidelity. The reason for this is that the fidelity is not very well suited to probe the variations in the individual components of quantum devices. There are often multiple ways to implement a device, sometimes with dramatically different susceptibilities to variations in the device's components [11], and it is not clear *a priori* how an array of fidelities associated with these different component variations should be combined into a single number that can be used to identify the best way to implement the device. Here, we use a method from quantum metrology to approach this problem, where the output

Pieter Kok: p.kok@sheffield.ac.uk

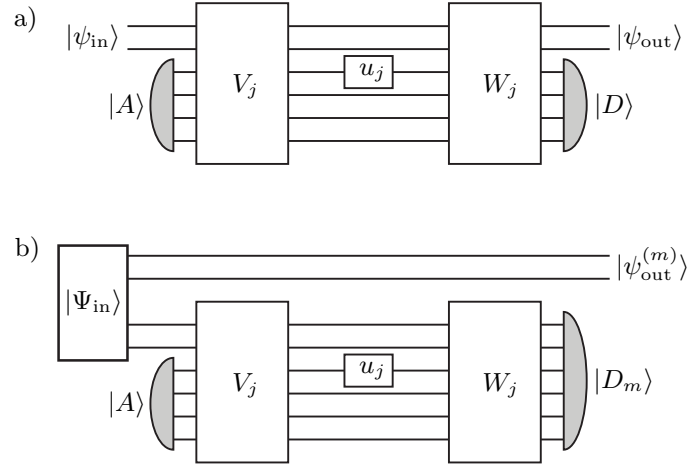


Figure 1: Decomposition of a quantum device into unitary components, specifically highlighting the component u_j . The horizontal lines may be qubits or optical modes, depending on the implementation. a) A gate $|\psi_{\text{out}}\rangle = \mathcal{U}_g|\psi_{\text{in}}\rangle$ with input state $|\psi_{\text{in}}, A\rangle$ and post-selected on a projection on $|D\rangle$; b) a quantum measurement device that has no output state, but gives a classical output “ m ”, indicated by the state $|D_m\rangle$. Entangling the input $|\psi_{\text{in}}\rangle$ with an auxiliary system prior to the device’s operation ($|\Psi_{\text{in}}\rangle$) allows us to apply the techniques for a) to measurements.

state of the quantum device carries information about the characteristics of the device’s components. This leads to the definition of the *sensitivity* of the device to variation in a component, and for a multi-component device we will obtain a sensitivity matrix. Together with a cost function for the different components, this sensitivity matrix provides a clear metric for the performance of different architectures for the same quantum device.

The paper is organised as follows: in section 2 we introduce the sensitivity for a device component. To realise this, we divide quantum devices into two categories, namely gates and measurement devices. The latter differs from the former in that there is no output state to the device. In section 3 we demonstrate how the sensitivity works for two incarnations of the nonlinear sign gate in linear optical quantum computing [11, 12], and for two implementations of the enhanced optical Bell measurement [13, 14]. In section 4 we bring together the sensitivities for different components into a single metric that tests different implementations of a quantum device, and we attempt to extract some general design principles for quantum technology architectures. We conclude our discussion in section 5.

2 Defining the *Sensitivity* for components of quantum devices

We wish to consider component sensitivity of two kinds of quantum devices. First, we consider quantum gates that have an input and an output, and which may be based on post-selection of auxiliary quantum systems (e.g., qubits or photons). This situation is depicted in Fig. 1a. As an example of this type of device, we will consider the nonlinear sign gate of linear optical quantum computing with photonic qubits [11, 12]. Second, we consider complex detection devices that use quantum gates to implement the desired observable. In this situation there is no surviving quantum state that can be used to track variations in components. To remedy this, we use entangled input states that allow us to define the action of a measurement in terms of a surviving quantum state [15]. This situation is depicted in Fig. 1b. As an example of this type of device, we will consider enhanced Bell measurements [13, 14].

2.1 Quantum Gates

Consider a quantum gate g described by the unitary evolution $|\psi_{\text{out}}\rangle = \mathcal{U}_g |\psi_{\text{in}}\rangle$, where the evolution can be post-selected using an auxiliary input state $|A\rangle$ and a detected state $|D\rangle$ (see Fig. 1). The detected state may be one of a family of states that herald a successful gate. The intervening evolution can often be decomposed in terms of N smaller unitary operations $U = \prod_{j=1}^N u_j$. These $u_j = \exp(-i\theta_j H_j)$ are the physical components of the quantum device. In general, their practical operation is more accurately described by a completely positive map that allows for imperfections in the device, but here we are interested in the ideal device and how deviations in the components affect the gate. While a more general discussion is certainly possible, it would also obscure some of the more intuitive aspects of this work.

After normalisation, the output of the device can be written as

$$|\psi_{\text{out}}\rangle = \frac{1}{\sqrt{p}} \langle D | U | \psi_{\text{in}}, A \rangle, \quad (2.1)$$

where $p = \|\langle D | U | \psi_{\text{in}}, A \rangle\|^2$ is the probability of success of the quantum device that implements the operation \mathcal{U}_g . Suppose we are interested in the j^{th} component of the device, denoted by u_j . Define

$$V_j = \prod_{k=1}^{j-1} u_k \quad \text{and} \quad W_j = \prod_{k=j+1}^N u_k. \quad (2.2)$$

Then we can decompose the output state as (see Fig. 1a):

$$|\psi_{\text{out}}\rangle = \frac{1}{\sqrt{p}} \langle D | W_j u_j V_j | \psi_{\text{in}}, A \rangle. \quad (2.3)$$

We can treat the sensitivity of the device to variations in u_j as an estimation problem of the parameter θ_j that characterises the component u_j . To this end we use the output state $|\psi_{\text{out}}\rangle$ as the basis for the estimation procedure. This state is already post-selected on the correct measurement outcome $\Pi_D \equiv |D\rangle\langle D|$. This is consistent with the operation of the gate, where the quantum computer trusts that upon getting the measurement outcome “ D ” the gate does what it is supposed to do.

Fortunately, we do not explicitly have to perform a complicated estimation procedure. Instead, we can calculate the average amount of information about θ_j that is contained in the output state $|\psi_{\text{out}}\rangle$. If the output state is very sensitive to variations in θ_j (the aspect we are trying to capture), then it must by definition vary strongly when the value of θ_j changes. The variation of the output state with θ_j is quantified by the quantum Fisher information $I_Q^{(j)}$, according to [16]

$$I_Q^{(j)} = \langle \dot{\psi}_{\text{out}} | \dot{\psi}_{\text{out}} \rangle - \left| \langle \psi_{\text{out}} | \dot{\psi}_{\text{out}} \rangle \right|^2, \quad (2.4)$$

where $|\dot{\psi}_{\text{out}}\rangle \equiv \partial_j |\psi_{\text{out}}\rangle$, the partial derivative of the output state with respect to θ_j . When we define

$$|\phi_{\text{in}}\rangle = u_j V_j |\psi_{\text{in}}, A\rangle \quad \text{and} \quad |\phi_{\text{out}}\rangle = W_j^\dagger |\psi_{\text{out}}, D\rangle, \quad (2.5)$$

the derivative of the output state is compactly written as

$$|\dot{\psi}_{\text{out}}\rangle = \frac{-i}{\sqrt{p}} \langle D | W_j H_j | \phi_{\text{in}} \rangle + \frac{1}{2} (\partial_j \log p) |\psi_{\text{out}}\rangle, \quad (2.6)$$

where H_j is the generator of translations in θ_j . We can then explicitly calculate the quantum Fisher information. First we calculate

$$\langle \dot{\psi}_{\text{out}} | \dot{\psi}_{\text{out}} \rangle = \frac{1}{p} \|\langle D | W_j H_j | \phi_{\text{in}} \rangle\|^2 + \frac{1}{4} (\partial_j \log p)^2 - p^{-\frac{1}{2}} (\partial_j \log p) \text{Im} \langle \phi_{\text{in}} | H_j | \phi_{\text{out}} \rangle, \quad (2.7)$$

and

$$\langle \psi_{\text{out}} | \dot{\psi}_{\text{out}} \rangle = \frac{-i}{\sqrt{p}} \langle \phi_{\text{out}} | H_j | \phi_{\text{in}} \rangle + \frac{1}{2} (\partial_j \log p) . \quad (2.8)$$

From this, we find that

$$I_Q^{(j)} = \frac{1}{p} \|\langle D | W_j H_j | \phi_{\text{in}} \rangle\|^2 - \frac{1}{p} |\langle \phi_{\text{out}} | H_j | \phi_{\text{in}} \rangle|^2 . \quad (2.9)$$

We can clean up this expression by inserting a resolution of the identity $\mathbb{I} = |\psi_{\text{out}}\rangle\langle\psi_{\text{out}}| + \sum_k |k\rangle\langle k|$ in the first term of $I_Q^{(j)}$, where the orthonormal states $|k\rangle$ complete $|\psi_{\text{out}}\rangle$ to form an orthonormal basis of the output Hilbert space. We find that

$$I_Q^{(j)} = \frac{1}{p} \sum_k |\langle \phi_k | H_j | \phi_{\text{in}} \rangle|^2 , \quad (2.10)$$

where we defined $|\phi_k\rangle \equiv W_j^\dagger |k, D\rangle$. We can understand this expression as the quadratic sum over the weak values of the generator H_j given the input state $|\psi_{\text{in}}, A\rangle$ and the output states $|k, D\rangle$ that are *orthogonal* to the intended output state $|\psi_{\text{out}}, D\rangle$. The success probability p of the quantum device is a common factor in $I_Q^{(j)}$ and does not play a role in the determination of the component sensitivity of a device (although it is important to include this factor when comparing the sensitivity of components in *different* devices with different p). In general, p changes when the component u_j changes, and this can in principle be used in an estimation procedure of θ_j . However, we post-select the state on the detection outcome Π_D , which means we have already discarded the information about the success rate of the quantum device. This is consistent with the normal operation of the gate \mathcal{U}_g .

The sensitivity S_j of the quantum device to components u_j can now be defined as

$$S_j \equiv \sum_k |\langle \phi_k | H_j | \phi_{\text{in}} \rangle|^2 . \quad (2.11)$$

While this is an elegant theoretical expression that gives a clear intuitive meaning for S_j , for practical purposes it may be beneficial to express S_j instead as

$$S_j = \langle \phi_{\text{in}} | H_j K_D H_j | \phi_{\text{in}} \rangle - |\langle \phi_{\text{out}} | H_j | \phi_{\text{in}} \rangle|^2 , \quad (2.12)$$

using $K_D = W_j^\dagger (\mathbb{I} \otimes \Pi_D) W_j$. This expression does not require the construction of the complementary basis states $|k\rangle$. It also holds for gates that rely on higher rank post-selection described by projectors Π_D , such as for example the double heralding procedure for creating entangled networks [17].

To determine a general, non-state-specific sensitivity of a device, we can average S_j over all possible input states. Alternatively, we can take as a standard input state an equal superposition of the eigenstates of \mathcal{U}_g , which is computationally much more straightforward.

2.2 Quantum Measurement Devices

Next, we consider quantum measurement devices, as shown in Fig 1b. The situation is slightly more complicated than the sensitivity for gate components, since there are typically multiple detection outcomes m , corresponding to projections onto $|D_m\rangle$ (which in turn are generally projections onto a subspace of the output space). The corresponding surviving quantum state $|\psi_{\text{out}}^{(m)}\rangle$ is defined by

$$|\psi_{\text{out}}^{(m)}\rangle = \frac{1}{\sqrt{p_m}} \langle D_m | U | \Psi_{\text{in}}, A \rangle , \quad (2.13)$$

where the input state $|\Psi_{\text{in}}\rangle$ is a maximally entangled state that allows us to relate the measurement outcome to an output state that can be used to define the sensitivity:

$$|\Psi_{\text{in}}\rangle = \frac{1}{\sqrt{d}} \sum_k |B_k, B_k\rangle , \quad (2.14)$$

with d the dimension of the input state space of the measurement device. The states $|B_k\rangle$ are the orthonormal eigenstates of the observable measured in the measurement device [15].

To calculate the sensitivity of the j^{th} component of the measurement device, parameterised by θ_j , we again calculate the quantum Fisher information of θ_j in the output state $|\psi_{\text{out}}^{(m)}\rangle$. Clearly, this will be different for different outcomes m , and we define the quantum Fisher information $I_Q^{(j,m)}$ for each component j and measurement outcome m . The total quantum Fisher information for the j^{th} component is then the weighted sum over all measurement outcomes

$$I_Q^{(j)} = \sum_{m \neq m_f} p_m I_Q^{(j,m)}. \quad (2.15)$$

One subtlety that we will encounter in the next section is that sometimes there are outcomes m_f of the measurement device that indicate the measurement has *failed* to produce a useful outcome. There may still be information in $|\psi_{\text{out}}^{(m)}\rangle$, but since these outcomes (and any post-selection based on these outcomes) are discarded in normal operation of the device, deviations in $|\psi_{\text{out}}^{(m_f)}\rangle$ have no effect on the device operation and we must *not* include $I_Q^{(j,m_f)}$ in the calculation of the sensitivity.

Proceeding with the calculation of $I_Q^{(j,m)}$, we use that

$$I_Q^{(j,m)} = \left\langle \dot{\psi}_{\text{out}}^{(m)} \left| \dot{\psi}_{\text{out}}^{(m)} \right\rangle - \left| \left\langle \dot{\psi}_{\text{out}}^{(m)} \left| \dot{\psi}_{\text{out}}^{(m)} \right\rangle \right|^2 \right. \quad (2.16)$$

Following the same method as in the previous section, we find that

$$I_Q^{(j,m)} = \frac{1}{p_m} \left\langle \phi_{\text{in}} \left| H_j W_j^\dagger (\Pi_m \otimes \mathbb{I}) W_j H_j \right| \phi_{\text{in}} \right\rangle - \left| \left\langle \phi_{\text{out}}^{(m)} \left| H_j \right| \phi_{\text{in}} \right\rangle \right|^2, \quad (2.17)$$

where Π_m is the projector onto the subspace associated with the state $|D_m\rangle$, which may have rank greater than one, and the states $|\phi_{\text{out}}^{(m)}\rangle$ and $|\phi_{\text{in}}\rangle$ are defined as

$$|\phi_{\text{in}}\rangle = u_j V_j |\Psi_{\text{in}}, A\rangle \quad \text{and} \quad |\psi_{\text{out}}^{(m)}\rangle = W_j^\dagger |\psi_{\text{out}}^{(m)}, D_m\rangle. \quad (2.18)$$

The unitary evolutions u_j , V_j and W_j are defined as in Fig. 1b. We can insert a resolution of the identity into the first term:

$$\mathbb{I} = |\psi_{\text{out}}^{(m)}\rangle \langle \psi_{\text{out}}^{(m)}| + \sum_k |\xi_k^{(m)}\rangle \langle \xi_k^{(m)}|, \quad (2.19)$$

for some orthonormal set $\{|\xi_k^{(m)}\rangle\}$ that span the subspace $\mathbb{I} - |\psi_{\text{out}}^{(m)}\rangle \langle \psi_{\text{out}}^{(m)}|$, and this leads to

$$I_Q^{(j,m)} = \frac{1}{p_m} \sum_k \left| \left\langle \phi_k^{(m)} \left| H_j \right| \phi_{\text{in}} \right\rangle \right|^2, \quad (2.20)$$

with $|\phi_k^{(m)}\rangle = W_j^\dagger |\xi_k^{(m)}, D_m\rangle$. The sensitivity then becomes

$$S_j = \sum_{k=1}^{d-1} \sum_{m \neq m_f} \left| \left\langle \phi_k^{(m)} \left| H_j \right| \phi_{\text{in}} \right\rangle \right|^2 = \sum_{k=1}^{d-1} \sum_{m \neq m_f} \langle \phi_{\text{in}} | H_j (\tilde{\Pi}_m \otimes \mathbb{I}) H_j | \phi_{\text{in}} \rangle, \quad (2.21)$$

where $\tilde{\Pi}_m \equiv W_j^\dagger \Pi_m W_j$. Two explicit examples of the beam splitter sensitivity of optical Bell measurements are given in section 3.2.

One may notice that the sensitivity, as measured by the quantum Fisher information, carries units of the inverse-squared of θ_j . When the θ_j refer to different components in a device, these units may be different, and a straight comparison will not be possible. Indeed, this is a key problem in constructing a single metric for different implementations of a quantum device, and we will return to this issue in section 4.

2.3 Variations in sources and detectors

The discussion so far has been restricted to unitary elements in a quantum device, but in practice we will also have to include variations in the auxiliary input states and the detectors. These can be included as unitary evolutions also. For example, an auxiliary input state $|A\rangle$ may be transformed into a different input state $|A(\theta_A)\rangle$ according to a unitary evolution

$$|A(\theta_A)\rangle = u_A(\theta_A)|A\rangle \quad \text{with} \quad u_A(\theta) = \exp\left(-\frac{i}{\hbar}H_A\theta_A\right), \quad (2.22)$$

where θ_A is the parameter associated with the evolution from $|A\rangle$ to $|A(\theta_A)\rangle$ generated by H_A . The choice of H_A is generally not unique, and must be chosen in accordance with the dynamics that governs the auxiliary system. In the ideal case, $\theta_A = 0$ and we recover the original auxiliary state. The sensitivity of the device to the auxiliary input state is then defined as

$$S_A = \langle \psi_{\text{in}}, A | H_A U^\dagger (\mathbb{I} \otimes \Pi_D) U H_A | \psi_{\text{in}}, A \rangle, \quad (2.23)$$

where $U = W_j u_j V_j$ is the unitary evolution defined in Eq. (2.1) and Fig. 1. Often, a physical imperfection in the source will lead to auxiliary input states that are mixed. We can accommodate these imperfections by extending the system to a larger, purifying Hilbert space. Formally, this extra Hilbert space can be included in the definition of $|A\rangle$ and $|D\rangle$.

Similarly, for imperfect detectors there is a way of calculating the sensitivity using the technique developed above. In the most general terms, an imperfect detector does not measure the exact observable M_D , but instead some rotated observable

$$M_D(\theta_D) = u_D M_D u_D^\dagger, \quad (2.24)$$

where $u_D = \exp(-iH_D\theta_D/\hbar)$ is the unitary evolution that rotates the eigenbasis of M_D to the eigenbasis of $M_D(\theta_D)$. The sensitivity of the device to detector imperfections is then defined as

$$S_D = \langle \psi_{\text{in}}, A | U^\dagger (\mathbb{I} \otimes H_D \Pi_D H_D) U | \psi_{\text{in}}, A \rangle. \quad (2.25)$$

Again, the choice of u_D is not unique and must be chosen in accordance with the dynamics that governs the detector.

3 Examples

To demonstrate the sensitivity measure, we consider several examples. We calculate the sensitivities to variations in the beam splitters in nonlinear sign (NS) gates for photonic linear optical quantum computing. These devices fall in the category of quantum gates. Next, we calculate the sensitivities to variations in the beam splitters in two types of optical Bell detectors, which fall in the category of quantum measurement devices. The dependence of optical gates on their constituent optical components has been studied before [18–23], but to our knowledge a unifying model for comparing implementations in arbitrary quantum device architectures has not yet been proposed.

3.1 The Nonlinear Sign gate in LOQC

The NS gate is a key component in the original proposal for linear optical quantum computing with photonic qubits by Knill, Laflamme and Milburn in 2001 [12]. It is a probabilistic gate that implements the unitary evolution

$$\alpha|0\rangle + \beta|1\rangle + \gamma|2\rangle \rightarrow \alpha|0\rangle + \beta|1\rangle - \gamma|2\rangle, \quad (3.1)$$

with $|n\rangle$ denoting single mode optical Fock states. The success probability is one quarter, and there are several inequivalent ways to implement the NS gate, two of which are shown in Fig. 2. The

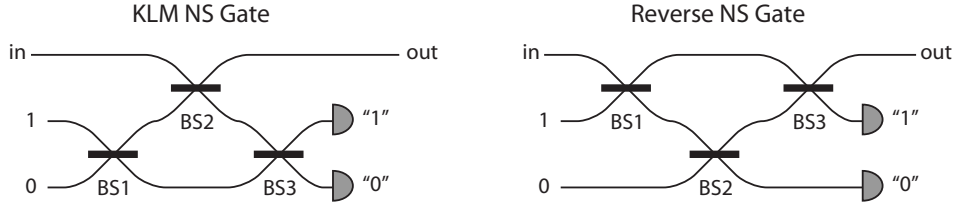


Figure 2: The nonlinear sign (NS) circuit for linear optical quantum computing. There are multiple versions of this circuit that are equivalent in terms of the success probability, number of optical elements, auxiliary photons and detectors, but they exhibit inequivalent behaviour in the presence of variations in the components. Here, we consider the KLM NS gate introduced in Ref. [12], and the Reverse NS gate introduced in Re. [11].

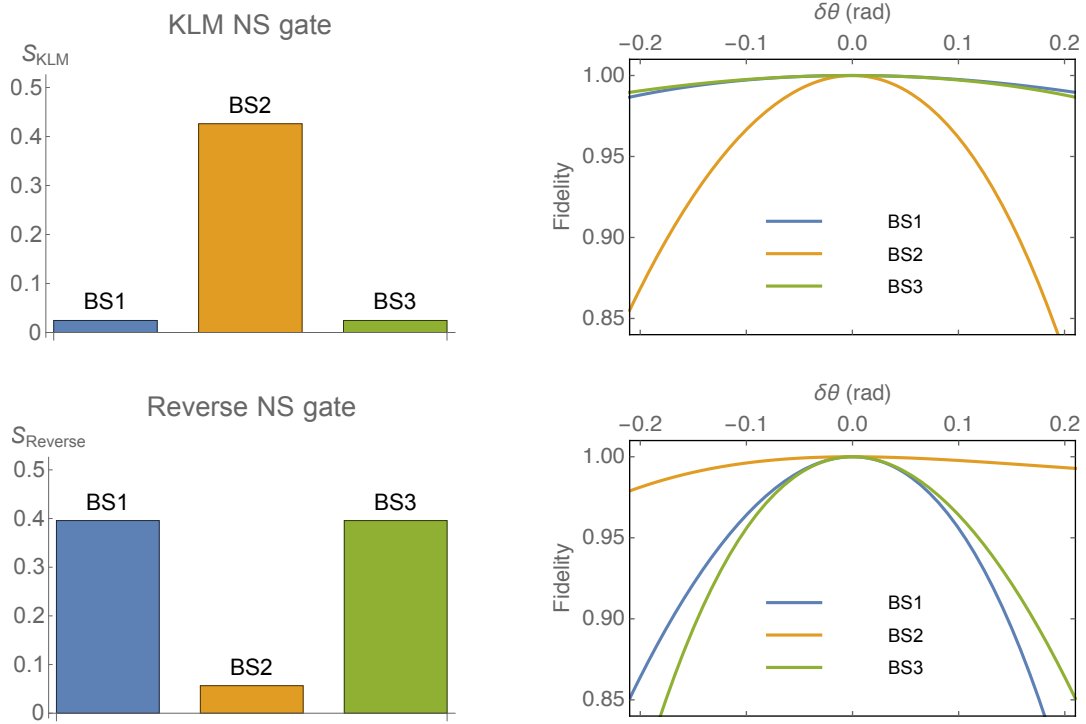


Figure 3: Sensitivities \bar{S}_{KLM} and \bar{S}_{Reverse} of the beam splitters in the KLM NS gate (left) and the Reverse NS gate (right), averaged over all input states. The units along the vertical axis are technically rad^{-2} , but are not important for the comparison of similar components in a gate. These results are consistent with the detailed analysis in Ref. [11].

beam splitter values in the two implementations are different, and we reported in Ref. [11] that the gate operation in the presence of variations in the beam splitter reflectivities depends strongly on the implementation.

For both the KLM and Reverse NS gate we choose the following description of the beam splitter operation acting on modes a_1 and a_2 :

$$\begin{pmatrix} \hat{b}_1 \\ \hat{b}_2 \end{pmatrix} = \begin{pmatrix} \cos \theta & \sin \theta \\ -\sin \theta & \cos \theta \end{pmatrix} \begin{pmatrix} \hat{a}_1 \\ \hat{a}_2 \end{pmatrix}, \quad (3.2)$$

where hats denote mode operators and θ is the defining parameter of the beam splitter. For the KLM

NS gate, the three beam splitter parameters θ_j are

$$\theta_1 = \arccos\left(\frac{1}{4 - 2\sqrt{2}}\right), \quad \theta_2 = \arccos\left(3 - 2\sqrt{2}\right) \quad \text{and} \quad \theta_3 = -\theta_1, \quad (3.3)$$

whereas for the Reverse NS gate, the three beam splitter parameters ξ_j are

$$\xi_1 = \arctan\left(\sqrt[4]{8}\right), \quad \xi_2 = \pi - \arctan\left(\frac{\sqrt{16\sqrt{2} - 13}}{7}\right) \quad \text{and} \quad \xi_3 = -\xi_1. \quad (3.4)$$

Both implementations use the same number of auxiliary photons and detections.

We calculate the sensitivity of the two NS gates to the various beam splitters. The results are shown in Fig. 3. Clearly, the sensitivity to variations in BS2 in the KLM NS gate is much greater than the sensitivity to variations in BS1 and BS3. This is reflected in the average fidelity of the output state of the KLM NS gate. By contrast, the sensitivity to variations in BS2 in the Reverse NS gate is much smaller than the sensitivity to variations in BS1 and BS3. Again, this is borne out in the average fidelities of the output state of the Reverse NS gate.

3.2 Enhanced linear optical Bell state detectors

Optical Bell measurements are an important tool in optical quantum information processing. They are used in a variety of applications, including teleportation [24–26], optical quantum computing [27], and quantum repeater proposals [28–30]. Originally, the optical Bell detector was introduced by Weinfurter [31] and Braunstein and Mann [32], and both schemes have a success probability of one half. In particular, these Bell detectors are capable of identifying the Bell states

$$|\Psi^\pm\rangle \equiv \frac{|H, V\rangle \pm |V, H\rangle}{\sqrt{2}}, \quad (3.5)$$

while they are completely incapable of distinguishing between the Bell states

$$|\Phi^\pm\rangle \equiv \frac{|H, H\rangle \pm |V, V\rangle}{\sqrt{2}}, \quad (3.6)$$

where $|H\rangle$ and $|V\rangle$ denote horizontally and vertically polarised photons, respectively. It was proved by Vaidman and Yoran [33] and Lütkenhaus, Calsamiglia, and Suominen [34] that optical Bell detectors without auxiliary photons have an upper bound of one half on the success probability. This severely increases the overhead of any practical application relying on these Bell detectors, since provisions must be made to ensure a failed Bell measurement does not negatively affect the operation of the quantum device (e.g., see the solution provided by the original proposal for linear optical quantum computing by Knill, Laflamme, and Milburn [12]).

A modification of the optical Bell detector was proposed by Grice [13], and Ewert & Van Loock [14], who suggested employing auxiliary photons to help distinguish between the remaining Bell states $|\Phi^\pm\rangle$. They showed that using one or two photon pairs increases the success probability to three quarters, and more generally, the use of n photons leads to a success probability of

$$p_{\text{Grice}}(n) = 1 - \frac{1}{n+2} \quad \text{and} \quad p_{\text{EVL}}(n) = 1 - \frac{1}{2^{n/2}}. \quad (3.7)$$

The circuits for the Grice and Ewert & Van Loock Bell detectors using two and four auxiliary photons, respectively, is given in Fig. 4. To obtain a success probability of one quarter, the Grice circuit requires a two-photon input state of the form

$$|\Phi^+\rangle = \frac{|H, H\rangle + |V, V\rangle}{\sqrt{2}}, \quad (3.8)$$

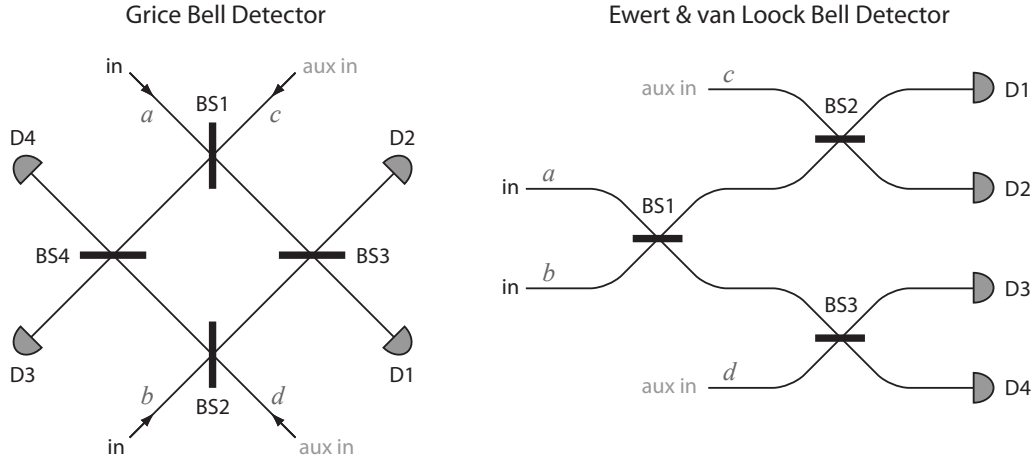


Figure 4: The entanglement-assisted Bell detection circuits of Grice and Ewert & van Loock. The Grice detector takes as input two photonic polarisation qubits and a polarisation Bell state $(|H, H\rangle + |V, V\rangle)/\sqrt{2}$ in the auxiliary input. Every mode carries a polarisation degree of freedom. The Ewert & van Loock Bell detector operates on dual-rail photonic qubits with auxiliary input states $(|2, 0\rangle + |0, 2\rangle)/\sqrt{2}$, but here we translated it to a polarisation implementation: each mode carries a polarisation degree of freedom. In this paper we consider only the sensitivity of the Bell detection circuits to beam splitter variations.

while the Ewert & van Loock circuit requires two two-photon input states in modes c and d of the form

$$|\Upsilon\rangle = \frac{|2H\rangle + |2V\rangle}{\sqrt{2}}. \quad (3.9)$$

Note that while the Ewert & van Loock circuit requires twice as many auxiliary photons to achieve the same success probability of three quarters as Grice's circuit, for higher success probabilities the Ewert & van Loock family of circuits is more efficient.

We calculate the sensitivity of the beam splitters in the Grice circuit, shown in Fig. 5. We choose as input to the quantum measurement device in Fig. 1b the state

$$|\Psi_{\text{in}}\rangle = \frac{1}{2}|\Phi^+, \Phi^+\rangle + \frac{1}{2}|\Phi^-, \Phi^-\rangle + \frac{1}{2}|\Psi^+, \Psi^+\rangle + \frac{1}{2}|\Psi^-, \Psi^-\rangle, \quad (3.10)$$

and we calculate the fidelity of the output state of the device with the expected Bell state due to the measurement outcome. The first two beam splitters that the input photons encounter (BS1 and BS2) exhibit a significantly lower sensitivity than the last two beam splitters (BS3 and BS4). This is corroborated by the fidelity of the output state.

For the Ewert & van Loock circuit we perform similar calculations, with the same input state in Eq. (3.10), and we find that it is the first beam splitter (BS1) that exhibits the greatest sensitivity. As expected, due to the symmetry of the circuit, beamsplitters BS2 and BS3 have the same sensitivity. The fidelity plots again confirm the sensitivities (see Fig. 6).

It is tempting to make a judgement, based on the above analysis, which NS gate or Bell detector is more suitable for implementation. However, in our examples we have only considered the sensitivities of the beam splitters, and we have not included variations in path lengths (or phases), auxiliary input states, or detector imperfections. These must all be taken into account before a value judgement can be made about a particular quantum device or gate implementation.

4 Device analysis based on the Sensitivity

The discussion has so far been restricted to sensitivities of individual components. However, in order to make a judgement on the best implementation of a quantum device, we would like to have a single

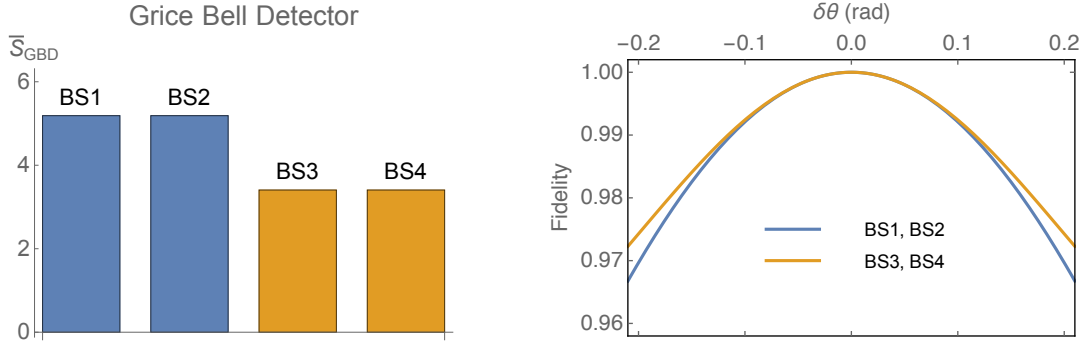


Figure 5: The beam splitter sensitivities of the Bell detection circuits of Grice, compared with the fidelities for the different beam splitter variations. Beam splitters BS1 and BS2 are entirely equivalent, as are BS3 and BS4. The sensitivities for BS1 and BS2 are 5.2, while the sensitivities for BS1 and BS2 are 3.4. The fidelities (right) reflect this sensitivity.

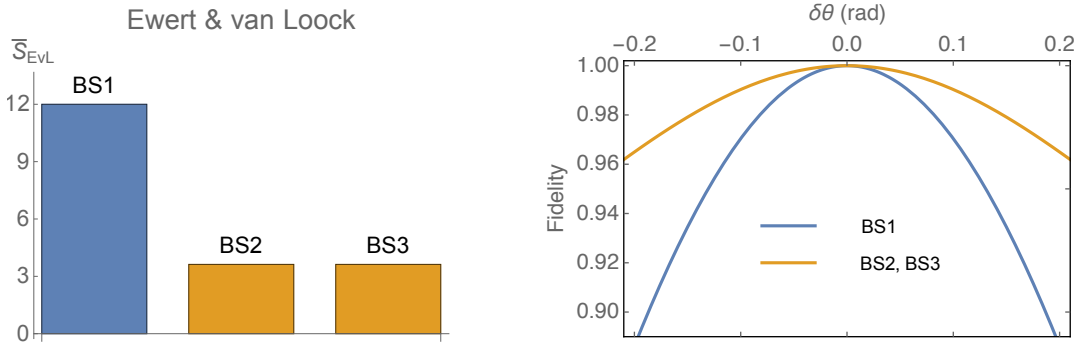


Figure 6: The beam splitter sensitivities of the Bell detection circuits of Ewert & van Loock, compared with the fidelities for the different beam splitter variations. Beam splitters BS2 and BS3 are equivalent. The sensitivity for BS1 is 12, while the sensitivities for BS2 and BS3 are 3.6. Again, the fidelities (right) reflect this sensitivity. In particular, the large sensitivity of the device to variations in BS1 is clear in the fidelity plot.

number characterising each implementation. At first sight, this seems impossible: how can we reliably force a multi-dimensional problem onto a one-dimensional scale? Especially when different component parameters have different units, comparing elements even within the same quantum device is comparing apples and oranges. To circumvent this problem, we may again use a technique from classical and quantum metrology. We can make a sensible judgement on the relative merits of implementations by introducing a cost function for the different components.

First, consider that the output state $|\psi_{\text{out}}\rangle$ (or $|\psi_{\text{out}}^{(m)}\rangle$ for measurement devices) depends in principle on a large array of parameters

$$\boldsymbol{\theta} = (\theta_1, \dots, \theta_M), \quad (4.1)$$

where M denotes the number of different components in the quantum device. In quantum metrology, for each output state $|\psi_{\text{out}}\rangle$ we assign a quantum Fisher information *matrix* that can be described by

$$[I_Q]_{jk} = 4 \operatorname{Re} [\langle \partial_j \psi_{\text{out}} | \partial_k \psi_{\text{out}} \rangle - \langle \partial_j \psi_{\text{out}} | \psi_{\text{out}} \rangle \langle \psi_{\text{out}} | \partial_k \psi_{\text{out}} \rangle], \quad (4.2)$$

where ∂_j and ∂_k are derivatives with respect to θ_j and θ_k , respectively. In turn, these are the parameters associated with the device components u_j and u_k . Calculating the derivatives as before, we obtain the matrix elements

$$[I_Q]_{jk} = \frac{4}{p} \operatorname{Re} \left[\left\langle \psi_{\text{in}}, A \left| V_j^\dagger u_j^\dagger H_j W_j^\dagger (\mathbb{I} - |\psi_{\text{out}}\rangle \langle \psi_{\text{out}}|) \otimes \Pi_D W_k H_k u_k V_k \right| \psi_{\text{in}}, A \right\rangle \right]. \quad (4.3)$$

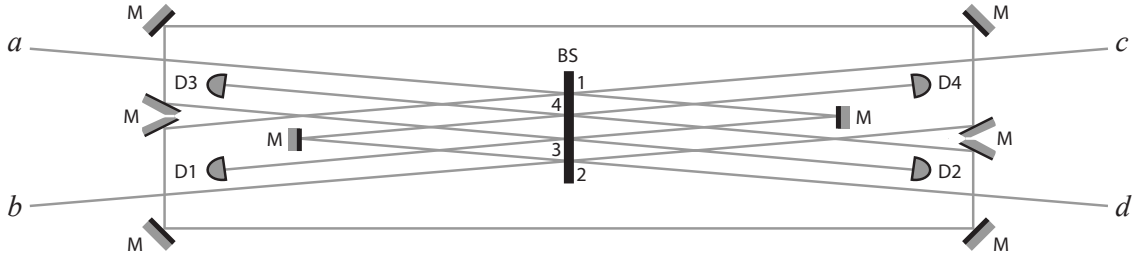


Figure 7: Similar to how a Mach-Zehnder interferometer can be folded into a Michelson-Morley interferometer, the Grice Bell detector can be folded onto only one beam splitter. This comes at the expense of adding several mirrors (M). The position of the inner mirrors can be adjusted to match the time of arrival of the photons at the detectors. Folding the circuit may reduce the overall sensitivity cost, depending on the added cost of the mirrors and the alignment.

Once we have a quantum Fisher information matrix, a bound on the covariance matrix of θ can be defined:

$$\text{Cov}(\theta) \geq I_Q^{-1}. \quad (4.4)$$

This is the famous quantum Cramér-Rao bound for multiple parameters [35], defined in the sense that $\text{Cov}(\theta) - I_Q^{-1}$ is a positive semi-definite matrix. The bound is tight if and only if the generators H_j are co-measurable [36]. The covariance bound can be cast into a simple inequality by introducing a family of real, symmetric cost matrices R :

$$\text{Tr}[R \text{Cov}(\theta)] \geq \text{Tr}[R I_Q^{-1}]. \quad (4.5)$$

The cost function serves to remove the units of the different matrix elements of $\text{Cov}(\theta)$ and I_Q^{-1} . Elements of R may denote the cost per beam splitter variation, or the cost per π -pulse variation in, e.g., a double-heralding entangling gate [17].

Now consider two quantum device implementations, \mathcal{J}_1 and \mathcal{J}_2 . We can calculate the sensitivity matrices $S(\mathcal{J}_1)$ and $S(\mathcal{J}_2)$ for these implementations, where as before $S = pI_Q$. Given two cost functions R_1 and R_2 , we say that implementation \mathcal{J}_1 is better than implementation \mathcal{J}_2 if

$$\text{Tr}[R_1 S(\mathcal{J}_1)^{-1}] < \text{Tr}[R_2 S(\mathcal{J}_2)^{-1}]. \quad (4.6)$$

We are forced to pick two different cost functions R_1 and R_2 when the components of the two implementations differ, and we must make sure that R_1 and R_2 are constructed using the same criteria. In other words, a beam splitter variation in \mathcal{J}_1 should carry the same cost as a beam splitter variation in \mathcal{J}_2 , etc. One cost function could be the identity matrix, where each component carries equal cost. This choice makes sense when there are no differences in units between the θ_j . Alternatively, the cost function could be a matrix with the actual economic cost per component. Such a choice is likely to favour devices with fewer components, such as the single beam splitter implementation of the Grice Bell detector shown in Fig. 7—although the added complexity of mirrors and alignment may wash out any gains from using fewer beam splitters. Note that the decision criterion in Eq. (4.6) typically depends on the choice of cost functions, unless one sensitivity matrix is always greater than the other.

We can make a simple comparison between the Grice Bell detector and the Ewert & van Loock Bell detector, where we take into account only the cost of beam splitter variations. While the Grice Bell detector employs more beam splitters, the beam splitters in the Ewert & van Loock Bell detector have a higher sensitivity. Comparing the implementations with a simple identity matrix cost function $R = \mathbb{I}$, we find that the Ewert & van Loock Bell detector has an overall sensitivity of $\text{Tr}[S(\mathcal{J}_{\text{EvL}})^{-1}] = 0.476$, and is therefore more resilient to beam splitter variations than the Grice Bell detector, which has an overall sensitivity of $\text{Tr}[S(\mathcal{J}_{\text{G}})^{-1}] = 0.731$. This shows that in this case, the design with fewer beam

splitters is preferable to the design with lower sensitivities to the beam splitter variations. One should bear in mind, however, that this analysis does not take into account phase changes due to path length differences and other mode matching or alignment issues.

When a device has more components than there are degrees of freedom in the output state, the quantum Fisher information matrix may become singular. In that case we cannot evaluate Eq. (4.6), and the method presented here does not provide a value for the overall sensitivity (and this device implementation may allow for significant simplifications). However, our method will still be able to provide valuable information about the relative importance of variations in the constituent components, and even when the sensitivity matrix is not singular, a full device analysis must include the consideration of the individual elements. This will inform us which components will produce the greatest improvements in the precision of the device when extra effort is spent on improvements.

The construction of quantum information processing devices is a challenging technical problem, and reducing sources of errors is an essential element of it. For each part of a device, quantum architecture designers should consider as many possible implementations as possible, and carry out a sensitivity analysis along the lines of the discussion presented here. This may be a lengthy task, and it is currently an open question whether we can construct guiding design principles that provide a shortcut to this task. Such principles would likely be highly implementation dependent.

5 Conclusions

We introduced a method for comparing different implementations of a quantum information processing device, including composite quantum gates and detectors, in terms of the sensitivity of the device to variations in its components. Our method is based on the amount of information about a component parameter is present in the output state. This is measured by the quantum Fisher information. For the examples considered here, we show that this method matches the predictions based on the fidelity of the device given variations in the components. The benefit of our method over the fidelity method is that we can collect the combined effect of variations in all components into a single overall sensitivity metric.

Acknowledgements

This research was funded in part by EPSRC's Quantum Communications Hub EP/M013472/1.

References

- [1] R. Raussendorf, J. Harrington, and K. Goyal, *New J. Phys.* **9**, 199 (2007).
- [2] R. Demkowicz-Dobrzanski, J. Kolodynski, and M. Guta, *Nature Commun.* **3**, 1063 (2012).
- [3] A. A. Uhlmann, *Rep. Math. Phys.* **9**, 273 (1976).
- [4] A. H. Myerson, D. J. Szwer, S. C. Webster, D. T. C. Allcock, M. J. Curtis, G. Imreh, J. A. Sherman, D. N. Stacey, A. M. Steane, and D. M. Lucas, *Phys. Rev. Lett.* **100**, 171 (2008).
- [5] C. J. Ballance, T. P. Harty, N. M. Linke, M. A. Sepiol, and D. M. Lucas, *Phys. Rev. Lett.* **117**, 060504 (2016).
- [6] J. Ghosh, A. Galiatdinov, Z. Zhou, and A. N. Korotkov, *Phys. Rev. A* **87** (2013), 10.1103/PhysRevA.87.022309.
- [7] L. H. Pedersen, N. M. Møller, and K. Mølmer, *Phys. Lett. A* **367**, 47 (2007).
- [8] J.-X. Cui and Z.-D. Wang, *Eur. Phys. J. D* **68**, 325 (2014).
- [9] M. Holzäpfel, T. Baumgratz, M. Cramer, and M. B. Plenio, *Phys. Rev. A* **91**, 401 (2015).
- [10] F.-Z. Kong, X.-L. Zong, M. Yang, and Z.-L. Cao, *Laser Phys. Lett.* **13** (2017), 10.1088/1612-2011/13/4/045201.
- [11] J. Crickmore, J. Frazer, S. Shaw, and P. Kok, *Phys. Rev. A* **94**, 022326 (2016).

- [12] E. Knill, R. Laflamme, and G. J. Milburn, *Nature* **409**, 46 (2001).
- [13] W. P. Grice, *Phys. Rev. A* **84**, 042331 (2011).
- [14] F. Ewert and P. van Loock, *Phys. Rev. Lett.* **113**, 140403 (2014).
- [15] P. Kok and S. L. Braunstein, *Phys. Rev. A* **63**, 033812 (2001).
- [16] S. L. Braunstein, C. M. Caves, and G. J. Milburn, *Ann. Phys.* **247**, 135 (1995).
- [17] S. D. Barrett and P. Kok, *Phys. Rev. A* **71**, 060310 (2005).
- [18] S. Glancy, J. M. LoSecco, H. M. Vasconcelos, and C. E. Tanner, *Phys. Rev. A* **65**, 062317 (2002).
- [19] T. C. Ralph, N. K. Langford, T. B. Bell, and A. G. White, *Phys. Rev. A* **65**, 062324 (2002).
- [20] A. P. Lund, T. B. Bell, and T. C. Ralph, *Phys. Rev. A* **68**, 022313 (2003).
- [21] P. P. Rohde, G. J. Pryde, J. L. O’Brien, and T. C. Ralph, *Phys. Rev. A* **72**, 032306 (2005).
- [22] P. P. Rohde, T. C. Ralph, and M. A. Nielsen, *Phys. Rev. A* **72**, 052332 (2005).
- [23] P. P. Rohde and T. C. Ralph, *Phys. Rev. A* **71**, 032320 (2005).
- [24] C. H. Bennett, G. Brassard, C. Crepeau, R. Jozsa, A. Peres, and W. K. Wootters, *Phys. Rev. Lett.* **70**, 1895 (1993).
- [25] D. Bouwmeester, J. Pan, K. Mattle, M. Eibl, H. Weinfurter, and A. Zeilinger, *Nature* **390**, 575 (1997).
- [26] P. Kok and S. L. Braunstein, *Phys. Rev. A* **61**, 042304 (2000).
- [27] D. E. Browne and T. Rudolph, *Phys. Rev. Lett.* **95**, 010501 (2005).
- [28] H. J. Briegel, W. Dür, J. I. Cirac, and P. Zoller, *Phys. Rev. Lett.* **81**, 5932 (1998).
- [29] W. Dür, H. J. Briegel, J. I. Cirac, and P. Zoller, *Phys. Rev. A* **59**, 169 (1999).
- [30] P. Kok, C. P. Williams, and J. P. Dowling, *Phys. Rev. A* **68**, 022301 (2003).
- [31] H. Weinfurter, *Eur. Phys. Lett.* **25**, 559 (1994).
- [32] S. L. Braunstein and A. Mann, *Phys. Rev. A* **51**, R1727 (1995).
- [33] L. Vaidman and N. Yoran, *Phys. Rev. A* **59**, 116 (1999).
- [34] N. Lütkenhaus, J. Calsamiglia, and K. A. Suominen, *Phys. Rev. A* **59**, 3295 (1999).
- [35] C. W. Helstrom, *Int. J. Theor. Phys.* **8**, 361 (1973).
- [36] S. Ragy, M. Jarzyna, and R. Demkowicz-Dobrzański, *Phys. Rev. A* **94**, 052108 (2016).